Metathesis Depolymerization for Removable Surfactant Templates

Timothy M. Long,[†] Blake A. Simmons,[‡] James R. McElhanon,[‡] Steven R. Kline,[§] David R. Wheeler,[∥] Douglas A. Loy,[⊥] Kamyar Rahimian,[∥] Thomas Zifer,[‡] and Gregory M. Jamison*,[†]

Electronic Materials and Nanostructured Materials Department, Sandia National Laboratories, Albuquerque, New Mexico 87185, Materials Chemistry Department, Sandia National Laboratories, Livermore, California 94551, NIST Center for Neutron Research, National Institute of Standards and Technology, Gaithersburg, Maryland 20899, Micro-Total-Analytical Systems Department, Sandia National Laboratories, Albuquerque, New Mexico 87185, and Materials Science and Engineering Department, University of Arizona, Tucson, Arizona 85721

Received June 1, 2005

Current methodologies for the production of meso- and nanoporous materials include the use of a surfactant to produce a self-assembled template around which the material is formed. However, post-production surfactant removal often requires centrifugation, calcination, and/or solvent washing which can damage the initially formed material architecture(s). Surfactants that can be disassembled into easily removable fragments following material preparation would minimize processing damage to the material structure, facilitating formation of templated hybrid architectures. Herein, we describe the design and synthesis of novel cationic and anionic surfactants with regularly spaced unsaturation in their hydrophobic hydrocarbon tails and the first application of ring closing metathesis depolymerization to surfactant degradation resulting in the mild, facile decomposition of these new compounds to produce relatively volatile nonsurface active remnants.

Introduction

A common strategy for preparing meso- and nanoporous materials involves surfactant-mediated synthesis wherein self-assembly of the surfactant provides a template around which the ultimate material is grown. Examples of such templated materials include the silicates MCM-41[1] and ZSM-5.[2] However, post-production thermal regimens for surfactant removal require calcination or hydrothermal treatments that can damage the initially formed material architecture. The effects of these processing conditions can include structural shrinkage,[3] microporous structure coalescence,[4] loss of mesotropically ordered structures,[5] introduction of structural defects,[6] or pore blockage resulting from the incomplete surfactant removal.[7] Additionally, organic and other nonsiliceous materials are often unstable under the severe thermal conditions (>500 °C) required for calcination.[8] Quantitative template removal remains a persistent problem; some organics have been shown to remain in templated materials such as MCM-41 at temperatures as high as 1000 °C.[9] Alternative surfactant removal processes, including supercritical CO_2 extraction,[10] microwave irradiation,[11] and O_3 oxidation,[12] produce improved materials with larger pores and narrower pore size distributions with respect to calcined materials; however, these methods are not ideal for large scale production or synthesis of templated organic "soft" materials due to the specialized equipment required (CO_2, microwaves) or involvement of highly reactive agents (O_3).

One method to address the issue of surfactant removal is to design surfactants which may be decomposed due to external chemical stimuli. Examples of surfactants which may be degraded under mild chemical conditions are few.[13] Generally, a change in the system pH has been used to degrade surfactants with acid-sensitive[14] functionalities such as dioxolanes.[15] This strategy has been successfully utilized for removal of detergents used in preparation of hydrophobic protein samples for MALDI-MS analysis.[16]

* To whom correspondence should be addressed. E-mail: gmjamis@sandia.gov.

[†] Electronic Materials and Nanostructured Materials Department, Sandia National Laboratories, Albuquerque.

[‡] Sandia National Laboratories, Livermore, California.

[§] National Institute of Standards and Technology.

[∥] Micro-Total-Analytical Systems Department, Sandia National Laboratories, Albuquerque.

[⊥] University of Arizona.

(1) (a) Kresge, C. T.; Leonowicz, M. E.; Roth, W. J.; Vartuli, J. C.; Beck, J. S. *Nature* **1992**, *359*, 710−712. (b) Beck, J. S.; Vartuli, J. C.; Roth, W. J.; Leonowicz, M. E.; Kresge, C. T.; Schmitt, K. D.; Chen, C. T.-W.; Olson, D. H.; Sheppard, E. W.; McCullen, S. B.; Higgens, J. B.; Schlenken, J. L. *J. Am. Chem. Soc.* **1992**, *114*, 10834−10843.

(2) Argauer, R. J.; Landolt, G. R. U.S. Patent No. 3,702,886, 1972.

(3) Chen, C.-Y.; Li, H.-X.; Davis, M. E. *Microporous Mater.* **1994**, *2*, 17−26.

(4) Lin, H.-P.; Mou, C.-Y. *Acc. Chem. Res.* **2002**, *35*, 927−935.

(5) Kruk, M.; Jaroniec, M.; Sayari, A. *Microporous Mesoporous Mater.* **1999**, *27*, 217−229.

(6) (a) Shen, S. C.; Kawi, S. *Langmuir* **2002**, *18*, 4720−4728. (b) Perez-Arevalo, J. F.; Dominguez, J. M.; Terres, E.; Rojas-Hernandez, A.; Miki, M. *Langmuir* **2002**, *18*, 961−964.

(7) Keene, M. T. J.; Gougeon, R. D. M.; Denoyl, R.; Harris, R. K.; Rouquerol, J.; Llewellyn, P. L. *J. Mater. Chem.* **1999**, *9*, 2843−2850.

(8) (a) Ciesla, U.; Fröba, M.; Stucky, G.; Schüth, F. *Chem. Mater.* **1999**, *11*, 227−234. (b) Huo, Q.; Margolese, D.; Ciesla, U.; Feng, P.; Gier, T. E.; Sieger, P.; Leon, R.; Petroff, P.; Schüth, F.; Stucky, G. D. *Nature* **1994**, *368*, 317−321. (c) Stein, A.; Fendorf, M.; Jarvie, T. P.; Mueller, K. T.; Benesi, A. J.; Mallouk, T. E. *Chem. Mater.* **1995**, *7*, 304−313.

(9) Hudson, M. J.; Trens, P. *Stud. Surf. Sci. Catal.* **2000**, *128*, 505−513.

(10) Kawi, S.; Lai, M. W. *Chem. Commun.* **1998**, 1407−1408.

(11) He, J.; Yang, X.; Evans, D. G.; Duan, X. *Mater. Chem. Phys.* **2003**, *77*, 270−275.

(12) Keene, M. T. J.; Denoyl, R.; Llewellyn, P. L. *Chem. Commun.* **1998**, 2203−2204.

(13) Holmberg, K., Ed.; *Novel Surfacants*; Marcel Dekker: New York, 1998; pp 333−358.

10.1021/la051438l CCC: $30.25 © 2005 American Chemical Society
Published on Web 08/23/2005

A recent report details the use of condensable surfactants developed for the production of templated organo-silicates, bearing masked functionalities whose latent interior surface is exposed by acid-catalyzed ester hydrolysis following condensation of the amphiphihlic template into a sol−gel matrix.[17] Conversely, base-sensitive[18] cleavable surfactants have been pursued, including β-ammonium ketones.[19]

Attempts to develop surfactants which are chemically robust, yet degradable by the introduction of an external stimulus, have yielded photosensitive azosulfonates[20] as well as surfactants degradable via ozonolysis.[21] Also, we have recently introduced a new class of thermally sensitive furan-maleimide surfactants which displays well-defined thermal degradation behavior to nonsurface active components as a result of the Diels−Alder behavior of the furan-maleimide linkage.[22]

Many of these systems have not succeeded in the complete degradation of all components into non-surface active elements when characterized by surface tensiometry, reflected by final surface tension values less than that of pure water.[15,21b] Gallardo et al.[23] have demonstrated the ability to reversibly manipulate interfacial surface tension through incorporation of redox-active ferrocenyl moieties. Recently, a disulfide-containing system has been developed which can be reduced under ambient conditions to the hydrophilic thiol.[24] In this case, surface tensiometry confirms that the surface tension of water can be recovered after surfactant degradation; however, the utility of this system is limited, as the length of the resulting alkylammonium thiol degradation products is sufficiently large to possess surface active character.

Recent advances in ruthenium-promoted ring-closing alkene metathesis[25] (RCM) as a powerful synthetic methodology inspired us to consider whether it could be applied to catalytic surfactant degradation. Although ring-closing metathesis has become a powerful tool for the efficient synthesis of highly functionalized cyclic alkenes,[26] use of the reaction for the degradation of materials has been scarce. Poly(alkenes), such as poly(isoprene)[27] and poly(butadiene),[28] have been shown to be degradable by olefin metathesis catalysts. In the case of poly(butadiene), solid-state exposure to benzylidene-bis(tricyclohexylphosphine)dichlororuthenium (Grubbs 1st generation catalyst) resulted in decomposition of the polymer into low molecular weight cyclic structures and telechelic oligomers. Decomposition of poly(butadiene) under an ethylene atmosphere promoted acyclic diene metathesis depolymerization (ADMET) resulting in the efficient formation of 1,5-hexadiene. Similar phenomena have even been noted in systems bearing low concentrations of isolated backbone double bonds.[29]

These examples of metathesis depolymerization proceed due to the negligible ring strain in the cyclohexene monomer (resulting in a ceiling temperature of −23 °C for poly(cyclohexene) in the presence of metathesis-active catalysts).[30] Although poly(cyclohexene) oligomers have been isolated with a tin/tungsten based catalyst if the catalyst is destroyed below the ceiling temperature, entropically driven de-oligomerization regenerates cyclohexene monomer above −23 °C in the presence of catalyst.

Given the need to address complete surfactant removal under mild conditions, an opportunity exists to identify and develop a surfactant system responsive to the action of a catalytic degradation agent. The characteristics of poly(cyclohexene) under metathesis conditions make it an attractive hydrophobic surfactant moiety, suitable for catalytic surfactant decomposition. Herein, we describe the design and synthesis of novel cationic and anionic surfactants with regularly spaced unsaturation in their hydrophobic hydrocarbon tails. We also describe the first application of catalytic ring-closing metathesis depolymerization to surfactant decomposition resulting in the production of multiple equivalents of relatively volatile, nonsurface active cycloalkene "monomers" and complementary small molecule remnants which are more suitable for removal under relatively mild thermal conditions or by the action of an appropriate solvent than the original surfactants themselves. This method demonstrates the potential of these surfactants as suitable templates for clean removal from delicate, ordered material systems.

Experimental Section

General Procedures. Materials. 6-Bromo-1-hexanol was purchased from Combi-Blocks (San Diego, CA) and used as received. Triphenylphosphine was obtained from Acros Chemical and used as received. 7-Bromo-1-heptene, n-BuLi (1.6 M in hexanes), THF (anhydrous, Sure-seal), acetonitrile (anhydrous, Sure-seal), NaI (anhydrous), KI (anhydrous), and LiI (anhydrous) were purchased from Aldrich Chemical (Milwaukee, WI) and used as received. First- and second-generation Grubbs' catalysts were purchased from Strem Chemical (Newburyport, MA) or Aldrich Chemical and used as received. Thermogravimetric data were collected on a Perkin-Elmer TGA 7 thermogravimetric analyzer at a temperature ramp rate of 10 °C/min under N_2. Elemental analyses were preformed by Desert Analytic (Tucson, AZ). HRMS were collected by the University of Arizona Mass Spectroscopy Facility (Tucson, AZ).

Preparation of Surfactants. 7-(Triphenylphosphonium)-hept-1-enyl iodide (1). To a solution of 7-bromo-1-heptene (19.47

(14) (a) Ono, D.; Masuyama, A.; Okahara, M. *J. Org. Chem.* **1990**, *55*, 4461−4464. (b) Jaeger, D. A.; Li, B.; Clark, T. C., Jr. *Langmuir* **1996**, *12*, 4314−4316. (c) Jaeger, D. A.; Wettstein, J.; Zafar, A. *Langmuir* **1998**, *14*, 1940−1941. (d) Piasecki, A.; Sokolowski, A.; Burczyk, B.; Gancarz, R.; Kotlewska, U. *Langmuir* **1997**, *13*, 1434−1439.

(15) Jaeger, D. A.; Sayed, Y. M. *J. Org. Chem.* **1993**, *58*, 2619−2627.

(16) (a) Caprioli, R. M.; Porter, N. A.; Norris, J. L. WIPO Patent 2002, WO 02/097393 A2. (b) Norris, J. L.; Porter, N. A.; Caprioli, R. M. *Anal. Chem.* **2003**, *75*, 6642−6647.

(17) Zhang, Q.; Ariga, K.; Okabe, A.; Aida, T. *J. Am. Chem. Soc.* **2004**, *126*, 988−989.

(18) (a) Jaeger, D. A.; Finley, C. T.; Walter, M. R.; Martin, C. A. *J. Org. Chem.* **1986**, *51*, 3956−3959. (b) Lindstedt, M.; Allenmark, S.; Thompson, R. A.; Edebo, L. *Antimicrob. Agents Chemother.* **1990**, *34*, 1949−1954.

(19) West, C. A.; Sanchez, A. M.; Hanon-Aragon, A.; Salazar, I. C.; Menger, F. M. *Tetrahedron Lett.* **1996**, *37*, 9135−9138.

(20) Mezger, T.; Nuyken, O.; Meindl, K.; Wokaun, A. *Prog. Org. Coat.* **1996**, *29*, 147−157.

(21) (a) Masuyama, A.; Endo, C.; Takeda, S.; Nojima, M. *Chem. Commun.* **1998**, 2023−2024. (b) Masuyama, A.; Endo, C.; Takenda, S.; Nojima, M.; Ono, D.; Takeda, T. *Langmuir* **2000**, *16*, 368−373.

(22) McElhanon, J. R.; Zifer, T.; Kline, S. R.; Wheeler, D. R.; Loy, D. A.; Jamison, G. M.; Long, T. M.; Rahimian, K.; Simmons, B. A. *Langmuir* **2005**, *21*, 3259−3266.

(23) (a) Gallardo, B. S.; Hwa, M. J.; Abbott, N. L. *Langmuir* **1995**, *11*, 4209−4212. (b) Gallardo, B. S.; Metcalfe, K. L.; Abbott, N. L. *Langmuir* **1996**, *12*, 4116−4124. (c) Bennett, D. E.; Gallardo, B. S.; Abbott, N. L. *J. Am. Chem. Soc.* **1996**, *118*, 6499−6505. (d) Gallardo, B. S.; Abbott, N. L. *Langmuir* **1997**, *13*, 203−208.

(24) Abbott, N. L.; Jong, L. I. U.S. Patent No. 6,600,076, 2003.

(25) Grubbs, R. H.; Miller, S. J.; Fu. G. C. *Acc. Chem. Res.* **1995**, *28*, 446−452.

(26) (a) Deiters, A.; Martin, S. F. *Chem. Rev.* **2004**, *104*, 2199−2238. (b) McReynolds, M. D.; Dougherty, J. M.; Hanson, P. R. *Chem. Rev.* **2004**, *104*, 2239−2258. (c) Diver, S. T.; Giessert, A. J. *Chem. Rev.* **2004**, *104*, 1317−1382. (d) Prunet, J. *Angew. Chem., Int. Ed. Engl.* **2003**, *42*, 2826−2830.

(27) Craig, S. W.; Manzer, J. A.; Coughlin, E. B. *Macromolecules* **2001**, *34*, 7929−7931.

(28) (a) Wagener, K. B.; Puts, R. D.; Smith, D. W., Jr. *Makromol. Chem., Rapid Commun.* **1991**, *12*, 419−425. (b) Watson, M. D.; Wagener, K. B. *J. Polym. Sci. A* **1999**, *37*, 1857−1861. (c) Watson, M. D.; Wagener, K. B. *Macromolecules* **2000**, *33*, 1494−1496.

(29) Coates, G. W.; Grubbs, R. H. *J. Am. Chem. Soc.* **1996**, *118*, 229−230.

(30) Patton, P. A.; Lillya, C. P.; McCarthy, T. J. *Macromolecules* **1986**, *19*, 1266−1268.

g, 110 mmol) in acetonitrile (400 mL) were added PPh_3 (27.53 g, 105 mmol) and KI (18.26 g, 110 mmol). The solution was heated at reflux under argon for 15 h. After cooling, the solids were filtered and the solvent removed in vacuo. Subsequent washing with cold diethyl ether (3×) yielded **1** (49.74 g, 97%). ^{1}H NMR (400 MHz, $CDCl_3$): δ 7.85−7.40 (m, 15H), 5.63 (m, 1H), 4.78 (m, 2H), 3.49 (m, 2H), 1.88 (m, 2H), 1.56 (m, 4H), 1.27 (m, 2H); ^{13}C NMR (100 MHz, $CDCl_3$): δ 138.2, 135.1, 133.5 (d, J_{C-P} = 40 Hz), 130.5 (J_{C-P} = 80 Hz), 117.8 (d, J_{C-P} = 320 Hz), 114.5, 33.0, 29.7 (d, J_{C-P} = 80 Hz), 28.1, 23.0 (J_{C-P} = 200 Hz), 22.2; Elem. Anal: Calcd. for $C_{25}H_{28}IP$: C, 61.74; H, 5.80. Found: C, 61.90; H, 5.96.

13-Iodotrideca-1,7-diene (2). Under an argon atmosphere, **1** (48.60 g, 100 mmol) and LiI (40.20 g, 300 mmol) were dissolved in THF (1.0 L, anhydrous) and cooled to 0 °C. n-BuLi (1.6 M, 62.5 mL, 100 mmol) was added dropwise and the solution became a clear, deep orange-red. The solution was stirred at 0 °C for 1 h, and then 6-bromo-1-hexanal (18.50 g, 103.3 mmol) was added dropwise. The color was quickly quenched to a pale yellow color, and the solution was allowed to warm to room temperature with stirring overnight. Silica gel was added to the reaction and THF removed in vacuo. The product was eluted through a short silica plug with hexanes to give **2** as a clear pale yellow liquid (28.93 g, 96%). ^{1}H NMR (400 MHz, $CDCl_3$): δ 5.80 (m, 1H), 5.37 (m, 2H), 5.00 (m, 2H), 3.17 (t, 2H, J = 7.0 Hz), 2.04 (m, 6H), 1.84 (m, 2H), 1.40 (m, 8H); ^{13}C NMR (100 MHz, $CDCl_3$): δ 139.2, 139.1, 130.8, 130.2, 130.1, 129.6, 114.4, 33.8, 33.6, 32.6, 32.5, 30.5, 30.3, 30.1, 29.6, 29.5, 29.3, 29.2, 28.8, 28.7, 28.6, 27.2, 27.1, 7.3, 7.2; Elem. Anal: Calcd. for $C_{13}H_{23}I$: C, 50.99; H, 7.57. Found: C, 50.82; H, 7.33.

13-(Triphenylphosphonium)trideca-1,7-dienyl iodide (3). Prepared according to the procedure for compound **1**, yielded **3** as a waxy solid (88% yield). ^{1}H NMR (400 MHz, $CDCl_3$): δ 7.90−7.60 (m, 15H); 5.80 (m, 1H), 5.31 (m, 2H), 4.95 (m, 2H), 3.61 (m, 2H), 2.10−1.80 (m, 8H), 1.40−1.25 (m, 8H); ^{13}C NMR (100 MHz, $CDCl_3$): δ 139.0, 135.2, 133.7 (d, J_{C-P} = 40 Hz), 130.7 (d, J_{C-P} = 40 Hz), 130.1, 129.7, 129.2, 118.0 (d, J_{C-P} = 320 Hz), 114.2, 33.6, 32.3, 32.0, 30.1 (d, J_{C-P} = 60 Hz), 29.1, 29.0, 28.5, 27.0, 26.7, 25.9, 23.1 (d, J_{C-P} = 200 Hz), 22.5; HRMS (FAB): Calcd. for $C_{31}H_{38}P^+$: 441.2706. Found 441.2729.

19-Iodononadeca-1,7,13-triene (4). Prepared according to the procedure for compound **2**, yielded **4** as a pale yellow liquid (88% yield). ^{1}H NMR (400 MHz, $CDCl_3$): δ 5.82 (m, 1H), 5.38 (m, 4H), 4.99 (m, 2H), 3.19 (t, 2H, J = 8 Hz), 1.99 (br m, 10H), 1.83 (m, 2H), 1.45−1.30 (m, 12H); ^{13}C NMR (100 MHz, $CDCl_3$): δ 139.2, 139.1, 130.8, 130.5, 130.4, 130.3, 130.0, 129.9, 129.5, 114.4, 33.8, 33.6, 3.4, 32.6, 32.5, 30.5, 30.3, 30.1, 29.5, 29.4, 29.3, 28.8, 28.7, 28.6, 27.3, 27.2, 27.1, 7.2, 7.1; HRMS (EI): Calcd. for $C_{19}H_{33}I$: 388.1627. Found: 388.1628.

19-(*N*,*N*,*N*-Trimethylammonium)nonadeca-1,7,13-trienyl iodide (5). 19-Iodononadeca-1,7,13-triene (**4**) (1.55 g, 4.0 mmol) was heated to reflux in 33 wt. % Me_3N in EtOH (20 mL) overnight. After cooling, excess Me_3N and solvent were removed in vacuo and the resulting solid washed with hexanes and dried in vacuo to yield **5** as a white solid (1.50 g, 84%). ^{1}H NMR (400 MHz, $CDCl_3$): δ 5.75 (m, 1H), 5.35 (m, 4H), 4.97 (m, 2H), 3.61 (m, 2H), 3.48 (s, 9H), 2.10−1.95 (m, 10H), 1.78 (m, 2H), 1.6−1.2 (m, 12H), 1.45 (m, 4H); ^{13}C NMR (100 MHz, $CDCl_3$): δ 139.1, 139.0, 131.1, 131.0, 130.5, 130.3, 130.2, 129.8, 129.7, 129.3, 129.2,,-128.8, 114.2, 67.0, 53.8, 33.6, 32.4, 32.2, 29.4, 29.3, 29.2, 29.1, 29.0, 28.5, 28.4, 27.2, 27.1, 27.0, 26.9, 25.7, 25.5, 23.2, 23.1; HRMS (FAB): Calcd. for $C_{22}H_{42}N^+$: 320.3312. Found: 320.3317.

7-(*N*,*N*,*N*-Trimethylammonium)hept-1-enyl iodide (5′). 7-Iodo-1-heptene (4.75 g, 21.2 mmol) was heated to reflux in 33 wt. % Me_3N in EtOH (80 mL) overnight. After cooling, excess Me_3N and solvent were removed in vacuo and the resulting solid washed with hexanes and dried in vacuo to yield **5′** as a white solid (5.89 g, 98%). ^{1}H NMR (400 MHz, $CDCl_3$): δ 5.75 (m, 1H), 4.97 (m, 2H), 3.61 (m, 2H), 3.47 (s, 9H), 2.07 (m, 2H), 1.76 (m, 2H), 1.45 (m, 4H); ^{13}C NMR (100 MHz, $CDCl_3$): δ 138.1, 115.0, 66.7, 53.4, 33.3, 28.3, 25.6, 23.0; HRMS (FAB): Calcd. for $C_{10}H_{22}N^+$: 156.1747. Found: 156.1748.

1,12-Bis(*N*,*N*,*N*-trimethylammonium)dodec-1,12-enyl diiodide (5″). 7-(*N*,*N*,*N*-Trimethylammonium)hept-1-enyl iodide (**5′**) (1.06 g, 3.75 mmol) and 1,3-bis-(2,4,6-trimethylphenyl)-2-imidazolidinylidene)dichloro(phenylmethylene) (tricyclohexylphosphine)ruthenium (Grubbs second generation catalyst) (168 mg, 0.2 mmol) were dissolved in dichloromethane under an argon atmosphere and stirred at room temperature for 17 h. The solvent was removed and the resulting solids washed successively with acetone, dichloromethane, and acetonitrile to yield **5″** as a white solid (1.35, 67%). ^{1}H NMR (400 MHz, DMSO-d_6): δ 5.75 (m, 1H), 4.97 (m, 2H), 3.61 (m, 2H), 3.47 (s, 9H), 2.07 (m, 2H), 1.76 (m, 2H), 1.45 (m, 4H); ^{13}C NMR (100 MHz, DMSO-d_6): δ 130.4, 130.0, 129.5, 65.0, 64.9, 52.0, 31.7, 31.3, 29.6, 29.4, 25.8, 25.2, 21.9, 21.5; HRMS (FAB): Calcd. for $C_{18}H_{40}N_2^{2+}$: 142.1596 (doublet-charged monoisotopic mass). Found: 142.1594.

19-(Triphenylphosphonium)nonadeca-1,7,13-trienyl iodide (6). Prepared according to the procedure for compound **1**, yielded **6** as a waxy solid (93% yield). ^{1}H NMR (400 MHz, $CDCl_3$): δ 7.90−7.60 (m, 15H), 5.82 (m, 1H), 5.38 (m, 4H), 4.95 (m, 2H), 3.73 (m, 2H), 2.10−1.80 (m, 12H), 1.40−1.25 (m, 12H); ^{13}C NMR (100 MHz, $CDCl_3$): δ138.7, 135.0, 134.9, 133.4 (d, J_{C-P} = 40 Hz), 130.4 (d, J_{C-P} = 80 Hz), 130.0, 129.9, 129.6, 129.5, 129.4, 128.9, 117.8 (d, J_{C-P} = 360 Hz), 114.0, 33.4, 32.2, 32.1, 31.8, 29.8 (d, J_{C-P} = 60 Hz), 29.6, 29.1, 29.0, 28.9, 28.8, 28.7, 28.2, 28.1, 26.9, 26.8, 26.5, 22.9 (d, J_{C-P} = 200 Hz), 22.3, 22.2, 22.1; Elem. Anal: Calcd. for $C_{37}H_{48}IP$: C, 68.30; H, 7.44. Found: C, 68.39; H, 7.59.

Diethyl Heneicosa-2,8,14,20-tetraenylmalonate (7). Under an argon atmosphere, **6** (8.72 g, 13.4 mmol) was dissolved in anhydrous THF (200 mL) and cooled to 0 °C. To this was added n-BuLi (1.6 M, 8.4 mL, 13.4 mmol) dropwise, and the solution became a clear deep orange-red. The solution was stirred at 0 °C for 1 h, and then diethyl(formylmethyl)malonate[31] (2.71 g, 13.4 mmol) was added dropwise. The color quickly quenched to a light pale yellow color, the cooling bath was removed, and the solution was allowed to stir at room temperature overnight. Silica gel was added to the reaction, and THF was removed in vacuo. The product was eluted through a short silica plug with 15:1 ethyl acetate: hexanes to give **7** as a clear, colorless liquid (1.99 g, 33%). ^{1}H NMR (400 MHz, $CDCl_3$): δ 5.80 (m, 1H), 5.45 (m, 2H), 5.30 (m, 4H), 4.96 (m, 2H), 4.17 (q, 4H, J = 7.2 Hz), 3.34 (t, 1H, J = 7.6 Hz), 2.64, 2.56 (each a t, 2H, J = 7.4 Hz), 2.10−1.90 (m, 12H), 1.50−1.30 (m, 12H), 1.25 (t, 6H, J = 7.2 Hz); ^{13}C NMR (100 MHz, $CDCl_3$): δ 169.2, 145.1, 144.6, 139.2, 139.1, 133.9, 133.2, 130.6, 130.5, 130.4, 130.3, 130.1, 130.0, 129.9, 129.8, 128.6, 125.5, 124.8, 119.4, 114.4, 61.5, 61.4, 52.4, 52.2, 33.9, 32.6, 32.5, 32.0, 29.5, 29.4, 29.3, 29.2, 29.1, 29.0, 28.7, 28.6, 28.5, 27.3, 27.2, 26.8, 14.2; HRMS (FAB): Calcd. for $C_{28}H_{47}O_4^+$: 447.3469. Found: 447.3464.

Heneicosa-2,8,14,20-tetraenyl Malonic Acid (8). 7 (1.77 g, 3.91 mmol) was dissolved in 1:1 EtOH:water (50 mL), and KOH (2.20 g, 10 eq.) was added. The cloudy solution was heated to reflux under argon overnight and became clear during heating. The reaction was cooled and the solvents removed in vacuo. Water was added to the solids and the solution acidified with 1 M HCl. The product was then extracted with dichloromethane and washed with water, 1 M HCl, and saturated NaCl. Drying over anhydrous $MgSO_4$ and removal of the solvent in vacuo yielded **8** (1.23 g, 81%) as a clear oil. ^{1}H NMR (400 MHz, $CDCl_3$): δ 11.10 (br s, 2H), 5.79 (m, 1H), 5.60−5.30 (m, 6H), 4.96 (m, 2H), 3.48 (t, 1H, J = 7.4 Hz), [2.71, 2.62] (pr t, 2H, J = 7.2 Hz), 2.10−1.90 (m, 12H), 1.45−1.30 (m, 12H); ^{13}C NMR (100 MHz, $CDCl_3$): δ 175.0, 139.3, 139.2, 135.0, 134.2, 130.7, 130.6, 130.4, 130.3, 130.2, 130.1, 129.9, 129.8, 124.6, 123.9, 123.8, 114.4, 52.2, 52.0, 33.9, 32.6, 32.5, 31.9, 29.6, 29.4, 29.3, 29.1, 29.0, 28.9, 28.7, 28.6, 27.4, 27.3, 27.2, 26.8; HRMS (FAB): Calcd. for $C_{24}H_{39}O_4^+$: 391.2843. Found: 391.2835.

Aqueous Surfactant Sample Preparation. Aqueous solutions of surface-active species were prepared by dissolving carefully weighed amounts of **5** and **9** in deionized water. The native surfactant **8** had limited solubility in water; thus, the anionic biscarboxylate potassium salt (denoted **9** in Scheme 2) was obtained by addition of stoichiometric KOH to enhance water solubility.

Dynamic Surface Tension. Surface tension measurements were conducted using a SensaDyne (Mesa, AZ) QC3000 dynamic surface tensiometer that utilizes the maximum bubble pressure method. The fundamental operating principles and theoretical considerations of this method are explained in detail elsewhere.[32]

(31) Lopez, F.; Castedo, L.; Mascarenas, J. L. *Org. Lett.* **2002**, *4*, 3683−3685.

Scheme 1. Synthesis of Oligocyclohexenyltrimethylammonium Iodide 5; (a) PPh_3, NaI (b) 1. n-BuLi, LiI, THF; 2. 6-bromo-1-hexanal (c) Me_3N, EtOH (d) Grubbs catalyst (2nd gen.)

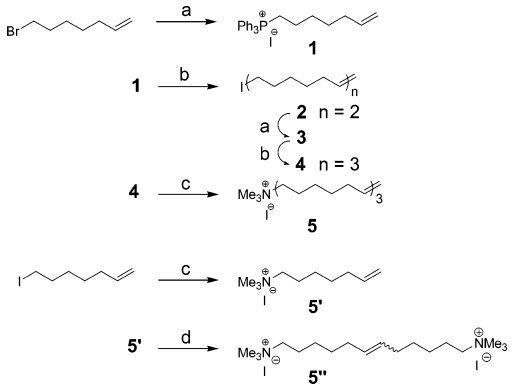

Scheme 2. Synthesis of Oligocyclohexenyl Malonic Acid 8 and Potassium Salt 9

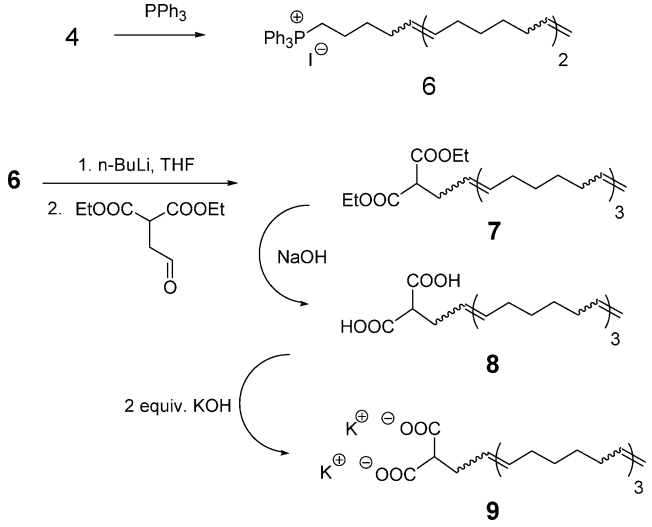

Two glass probes with different orifice diameters (0.5 and 4.0 mm) were submerged in an aqueous surfactant solution and nitrogen was bubbled through the samples. Dry nitrogen was used as the bubble source and was delivered at the slowest recommended bubble rate (0.5 Hz) possible for this instrument in order to approximate equilibrium surface tension values for each sample. The differential pressure is related to the interfacial surface tension of the liquid and gas. Surface tension calibration was carried out by measuring the surface tension of deionized water and ethanol and comparing that to known literature values. The solution temperature was monitored with a calibrated thermistor (±0.1 °C) attached to the orifice probes. Instrumental calibration was conducted for every change in experimental conditions and after prolonged periods of instrumental quiescence. All experiments were conducted at 26.0 ± 0.2 °C unless otherwise noted. Data were recorded for all experiments via a computer interface using the SensaDyne QC3000 version 5.3 software.

To demonstrate the decomposition of the surfactants in aqueous solution, an argon purged drybox was employed to protect the oxygen sensitive catalyst during decomposition. [1,3-Bis-(2,4,6-trimethylphenyl)-2-imidazolidinylidene] dichloro(phenylmethylene) (tricyclohexylphosphine)ruthenium (Grubbs 2nd generation catalyst) was introduced (30 mol %) under Ar to an aqueous solution of **5** (3 mM) or **9** (10 mM) and stirred rapidly. At specific time intervals, an aliquot was removed from the box and filtered through a 0.2 μm filter, and the surface tension measured as above.

Dye Solubilization. To investigate the enhanced solubility of a water-insoluble dye in the presence of micelles, excess amounts (0.02 g per 10 mL of aqueous sample) of Orange OT were added to separate concentration series of aqueous surfactant solutions and sonicated for 30 min in a water bath sonicator operated under ambient conditions. The solutions were allowed to settle under ambient conditions for 2 h and subsequently filtered using 0.2 μm PVDF syringe filters (Whatman) into 1 cm path length quartz cuvettes (3.5 mL, Starna Cells, Inc.). The amount of dye solubilized in each sample was measured by monitoring the absorbance intensity of each at 523 nm with a Shimadzu (Pleasanton, CA) 2401-PC UV−Vis Dual Beam Spectrophotometer operating at ambient conditions.

Small-Angle Neutron Scattering. Small-angle neutron scattering (SANS) experiments were performed at the NG3 beamline at the NIST Center for Neutron Research (NCNR) in Gaithersburg, MD. The measurements determined the absolute scattering intensity $I(q)$ as a function of the wave-vector q (= $[4\pi/\lambda]\sin[\theta/2]$, where λ is the incident neutron wavelength and θ the scattering angle). The q range for these experiments was set to cover the range of 0.003−0.19 Å^{-1}, the neutron wavelength was set at 10 Å, and the sample-to-detector distance was set to 10 and 1.9 m in order to encompass the stated q range. Sample concentrations were held constant at 3 mM for **5** and 10 mM for **9** dissolved in D_2O, which served as the neutron scattering contrast element. Samples were placed in quartz cells with a path length of 1 mm. The SANS data obtained were fitted using software programs developed at NCNR, which allows for various models to be tested covering a wide range of micellar geometries (i.e. vesicles, spheres, cylinders, disks, prolates, etc.). It was determined that the polydisperse cylinders model and the bimodal polydisperse hard sphere model were the best possible model fits to the data obtained from **5** and **9**, respectively.

Results and Discussion

1. Synthesis. A. Cationic Ammonium Surfactants. Cationic surfactants **5** and **9** (Schemes 1 and 2) were designed under the principle that they would decompose under ring-closing metathesis conditions into small cyclic molecules and an acyclic remnant containing the polar headgroup upon introduction of an appropriate catalyst. The hydrophobic tail of **5** and **9** was constructed with a C−C double bond positioned every seven bonds in order to permit thermodynamically favorable RCM de-oligomerization to cyclohexene. The metathesis behavior of cyclohexene dictates that alternative chemistries not involving cyclohexene as a precursor will be required.

The oligo(cyclohexene) tail section was synthesized as shown in Scheme 1. Triphenylphosphonium iodide **1** was prepared from 7-bromo-1-heptene with PPh_3 and NaI in acetonitrile. The in situ Finkelstein reaction followed by the addition of PPh_3 greatly increased the reaction rate and yield. Subsequent Wittig condensation of the ylide of **1** with 6-bromo-1-hexanal (prepared by PCC oxidation of 6-bromo-1-hexanol)[33] in the presence of LiI gave iodide **2** containing 5−8% (by ^{1}H NMR and gas chromatography) of the bromide endgroup. Although this mixture was satisfactory to continue with the synthesis, pure iodide **2** was readily obtained by treatment of the mixture with NaI in acetone. Repetition of the previous steps gave iodononadecatriene **4** in an overall 69% yield from 7-bromo-1-heptene. Amine quaternization was readily achieved through reaction of **4** with trimethylamine to generate oligocyclohexenyl trimethylammonium iodide **5** in 84% yield. For comparison purposes with surfactant decomposition products (vide infra), **5′** was prepared identically from 7-iodo-1-heptene and trimethylamine in 98% yield.

(32) (a) Manglik, R. M.; Wasekar, V. M.; Zhang, J. *Exp. Thermal Fluid Sci.* **2001**, *25*, 55−64. (b) Renouf, P.; Hebrault, D.; Desmurs, J.-R.; Mercier, J.-M.; Mioskowski, C.; Lebeau, L. *Chem. Phys. Lipids* **1999**, *99*, 21−32.

(33) Hon, Y.-S.; Chang, F.-J.; Lu, L.; Lin, W.-C. *Tetrahedron* **1998**, *54*, 5233−5246.

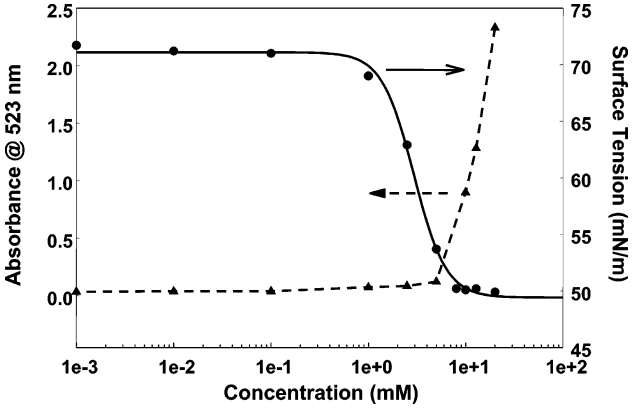

Figure 1. CMC determination for anionic surfactant **9** (● = surface tension; ▲ = dye solubilization).

B. Anionic Surfactants. For the headgroup of surfactant **9**, we chose an acetalaldehyde functionalized diethylmalonate as shown in Scheme 2.[34] To attach the surfactant tail via one final Wittig condensation, **4** was reacted with triphenylphosphine to give **6** in 93% yield. Addition of the ylide of **6** to (formylmethyl)malonic acid diethyl ester gave the diethyl malonate, **7** (33% yield), which can be readily hydrolyzed to free malonic acid **8** with NaOH in an ethanol/water mixture in 81% yield. Addition of two equivalents of KOH cleanly yielded the desired surfactant **9**. This system places an olefinic group one methylene removed from the headgroup (ensuring small molecule products) and places an additional alkene in the tail of the surfactant compared to the cationic ammonium system, which will produce an extra equivalent of cyclohexene upon surfactant degradation.

2. Physico-Chemical Behavior of Surfactants. Characterization of the surface active properties of aqueous solutions of **5** and **9** includes determination of the critical micelle concentration (CMC; that surfactant concentration at which spontaneous organization into micellar structures occurs) by surface tensiometry via the maximum bubble pressure method.[35] When conducted at very slow bubble rates, this method approximates static equilibrium conditions.[36] As the surfactant concentration is increased to that near the CMC range, the surface tension of the aqueous solution decreases below that of pure water (72.1 mN/m at 25 °C) and ultimately reaches a constant lower value beyond the CMC range, which is characteristic for a given surfactant exhibiting micellar aggregation.

Typically, long saturated alkyl chain carboxylate surfactants (hydrophobic chain length ≥ C_{20}) are insoluble in water.[37] The bis-carboxylate headgroup of **9** has the advantage of increasing the overall solubility of the surfactant in water as compared with mono-anionic carboxylate salts. Additionally, the inclusion of unsaturation in the hydrocarbon tail serves to increase solubility in water as well.[38] Consequently, with an unsaturated C_{21} chain and a dual-headed anionic group, water solubility of **9** was readily maintained. Surface tensiometry of a solution of **9** (Figure 1) determined the CMC surface tension to be 50 mN/m with a measured CMC of 5.9 mM. For comparison, simple, saturated-C_{18} containing soaps with a single carboxylic acid headgroup have CMCs around 1.8 mM; use of an unsaturated-C_{18} oleate tail slightly increases the CMC to 2.0 mM. Under the same conditions, the CMC surface tension of an aqueous solution of cationic ammonium surfactant **5** (Figure 2) was found to be 35 mN/m, with a measured CMC of 1.9 mM.

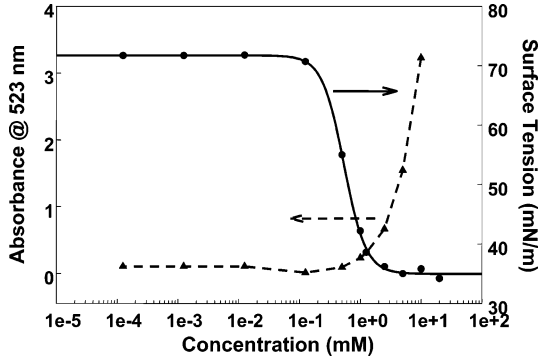

Figure 2. CMC determination for cationic surfactant **5** (● = surface tension; ▲ = dye solubilization).

Both surfactants **5** and **9** are stable in solution; upon standing for over 14 days at room temperature, we observed no change in the optical clarity or turbidity of a 10 mM solution of either surfactant (above the CMC for each). In addition, we observe less than a 5% change in the equilibrium surface tension of these over that time period.

Dye solubilization[39] was used to corroborate the CMC values obtained through surface tensiometry. Water-insoluble Orange OT was added to solutions of varying concentrations of **5** and **9** in water. At the concentration where micelles begin to form, the dye dissolves into the oily core of the micelle; the resulting change in Orange OT absorption (UV−vis spectroscopy) at 523 nm indicates a CMC value. In the case of **5**, this method yielded a CMC value of 1.2 mM. This compares favorably with saturated straight-chained analogues; for example, n-$C_{16}H_{33}N(Me)_3$-Br has a CMC of 0.9 mM[40] (the higher CMC value of **5** reflects the slightly greater hydrophilic nature of the unsaturated tails of surfactant **5**). Likewise, **9** was found to have a CMC of 4.7 mM. The CMC values obtained through this technique are therefore observed to be in good agreement with those obtained above. The slight discrepancy between them is attributed to the fact that the dye solubilization technique is a static probe of the micellar environment, whereas the surface tension is a dynamic probe.

The micellar geometric structure can be predicted based on the volumes occupied by the hydrophilic headgroup of the surfactant with respect to the volume of the hydrophobic tail.[41] The volume of the hydrophobic group in the core (V_H), cross-sectional area occupied by the headgroup (a_0), and length of the hydrophobic group in the core (l_c) can be employed in the empirical relationship

$$q = V_H/a_0 l_c \qquad (1)$$

to predict the micellar shape of a given surfactant in

(34) Groth, T.; Meldal, M. *J. Comb. Chem.* **2001**, *3*, 34−44.
(35) (a) Sugden, S. *J. Chem. Soc.* **1922**, *121*, 858−866. (b) Anacker, E. W. *Cationic Surfactants*; Marcel Dekker: New York, 1970; pp 203−88.
(36) Woolfrey, S. G.; Banzon, G. M.; Groves, M. J. *J. Colloid Interfacial Sci.* **1986**, *112*, 583−587.
(37) Porter, M. R. *Handbook of Surfactants*; Blackie: Glasgow, 1991; pp 54−59.
(38) Rosen, M. J. *Surfacants and Interfacial Phenomena*, 2nd ed.; Wiley: New York, 1989; pp 1−32.
(39) Holmberg, K., ed.; *Handbook of Applied Surface and Colloid Chemistry*; Wiley: Chichester, U.K., 2002; pp 239−249.
(40) Czerniawski, M. *Rocz. Chem.* **1966**, *40*, 1935−1945.
(41) (a) White, L. R.; Israelachvili, J. N.; Ninham, B. W. *J. Chem. Soc., Faraday Trans. 1* **1976**, *72*, 2526−2536. (b) Israelachvili, J. N.; Mitchell, D. J.; Ninham, B. W. *Biochim. Biophys. Acta* **1977**, *470*, 185−201. (c) Mitchell, D. J.; Ninham, B. W. *J. Chem. Soc., Faraday Trans. 2* **1981**, *77*, 601−629.

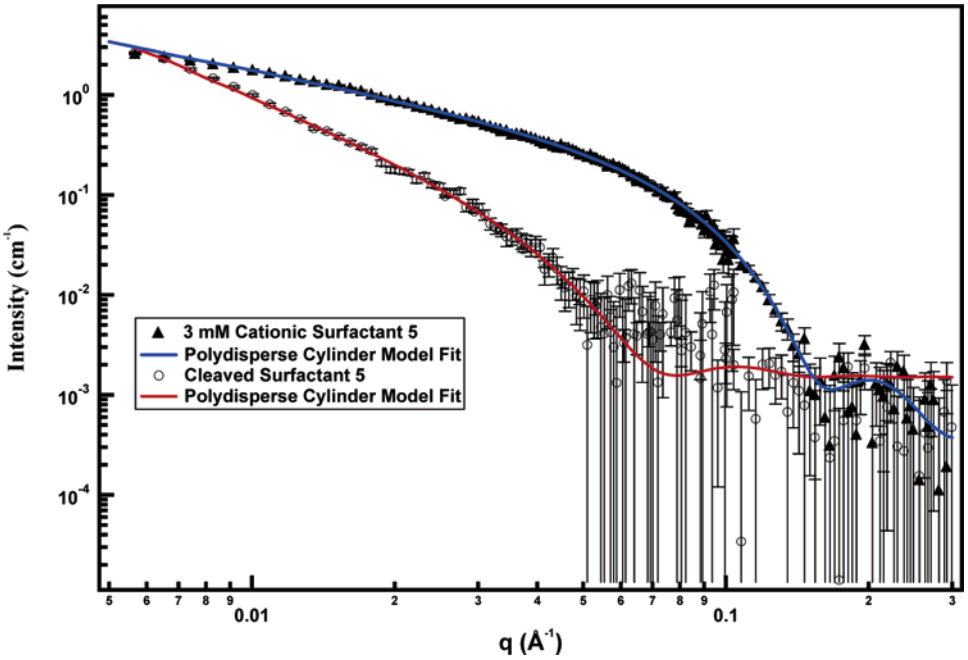

Figure 3. Small-angle neutron scattering spectra taken from 3 mM solutions of the cationic surfactant **5** before and after the introduction of 30 mol % Grubbs catalyst. Model fits from a polydisperse cylinder algorithm are shown as solid lines in each plot. Surfactants were dissolved in D_2O to provide contrast.

Table 1. Physicochemical Properties of the Surfactants 5 and 9

	CMC[a] (mM)	CMC[b] (mM)	γ_{cmc} (mN/m)	G (mol/cm^2)	a_{HG} (Å^2)	$\Delta G°_{mic}$ (kJ/mol)
5	1.9	1.2	35.3	1.94×10^{-10}	85.6	−25.5
9	5.9	4.7	50.1	1.42×10^{-10}	116.6	−22.2

[a] As determined by surface tensiometry. [b] As determined by Orange OT dye solubilization.

solution. Values for q of less than 0.33 typically yield spherical micelles, whereas values between 0.33 and 0.5, 0.5−1.0, and greater than 1 yield cylindrical, lamellar, and inverse micelles, respectively.

The physicochemical properties of a surfactant change to a significant degree after reaching the CMC due to the presence of the micelles and a surfactant saturated air−water interface.[42] The surface excess concentration (Γ) and the area per molecule at the interface (a) have been determined using the standard Gibbs equation simplified for dilute ($<10^{-2}$ M) ionic surfactant solutions given as[43]

$$\Gamma = -\frac{1}{4.6RT}\left(\frac{\mathrm{d}\gamma}{\mathrm{d}\log C}\right)_T \qquad (2)$$

and

$$a = \frac{10^{16}}{N_A\Gamma} \qquad (3)$$

where R is the gas constant, T the temperature at which the measurements were made (26 ± 0.2 °C), γ the surface tension, C the surfactant concentration, and N_A Avogadro's number.

In the case of **9**, a value of 116.6 Å^2 was calculated for the cross-sectional area of the headgroup (a_0, Table 1). Generally, anionic surfactants with a single carboxylate headgroup have cross-sectional areas of 40−50 Å^2 for their sodium salts. The larger cross-sectional area in the case of **9** is consistent with the larger potassium cation as well as the dual-headed nature of the headgroup. The volume of the hydrophobic core was calculated from the empirical relationship[44] $V_H = 27.4 + 26.9n$ Å^3, where n is the number of carbons in the hydrophobic tail (n = 21), yielding a value of V_H = 592.3 Å^3. The length of the hydrophobic chains in the tail can be approximated from MM2 calculations.[45] Since the regiochemistry of the alkenes in **9** are not absolute, all combinations of *cis*- and *trans*-alkenes can be assumed to be present. The extremes of these are represented by the all-cis and all-trans containing chains, yielding a range for l_c values of 19.5−24.9 Å. These values for l_c give q values of 0.20−0.26, within the range which would predict simple spherical micelles to be formed by **9** in aqueous solutions.

In the case of **5**, a value of 85.6 Å^2 was found for the cross-sectional area of the headgroup. This (a_0) is in good agreement with the cross-sectional areas of alkyltrimethylammonium surfactants, as the chloride or bromide salts have cross-sectional areas of 40−60 Å^2; however, the slightly larger value is attribute to the larger iodide anion. The volume of the hydrophobic core (V_H) for a C_{19} tail yields a value of 538.5 Å^3. MM2 calculations yielded extremes for the all-cis and all-trans containing hydrophobic tails (l_c) of 14.5−22.9 Å. These l_c values give q values of 0.27−0.43, which bridges the value range given for spherical and cylindrical morphologies.

Small-angle neutron scattering (SANS) experiments were conducted in an attempt to verify (in the case of **5**, to clarify) absolute micellar size and shape for both surfactant types. A SANS spectrum for a 3 mM solution of **5** in D_2O exhibited a traditional profile found for cylinders (Figure 3), and the data was successfully fit with a model developed for polydisperse cylinders. Similarly, a 10 mM solution of **9** in D_2O produced a SANS profile typical of polydisperse spheres (Figure 4), and a Schulz sphere model was successfully applied to the data. The

(42) Lange, R. K. *Surfactants: A Practical Handbook*; Hanser-Gardner: Cincinnatti, 1999; pp 13−25.
(43) Rosen, M. J. *Surfactants and Interfacial Phenomena*, 2nd ed.; Wiley-Interscience: New York, 1989; pp 65−68.
(44) Tanford, C. *The Hydrophobic Effect*, 2nd ed.; Wiley: New York, 1980.
(45) See the Supporting Information.

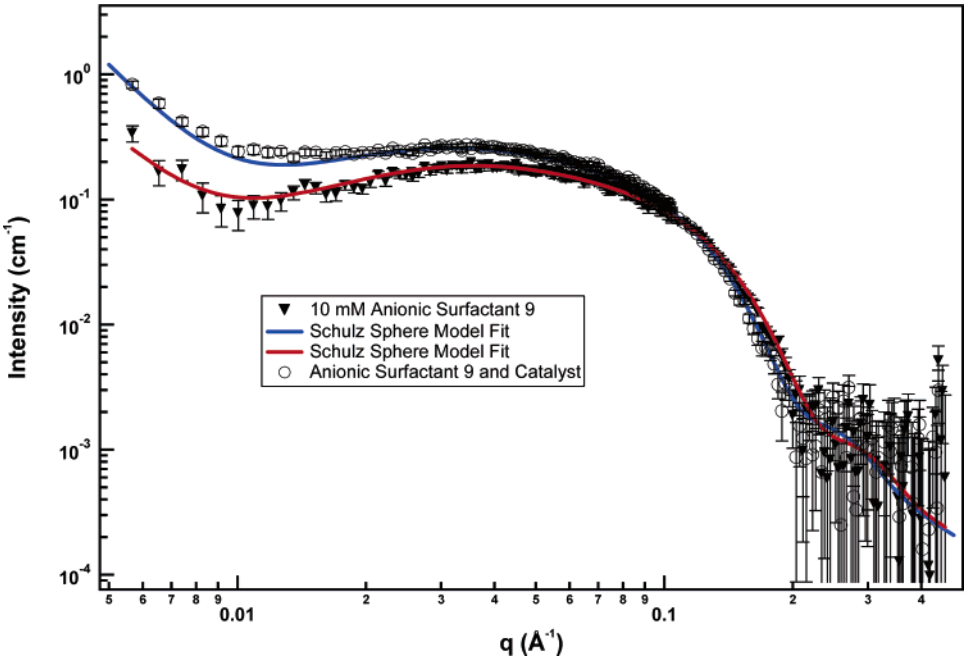

Figure 4. Small-angle neutron scattering spectra taken from 10 mM solutions of the anionic surfactant **9** before and after the introduction of the Grubbs catalyst. Model fits from a Schulz sphere algorithm are shown as solid lines in each plot. Surfactants were dissolved in D_2O to provide contrast.

Table 2. Micelle Dimensions Obtained from SANS Data of 5 and 9 before and after the Addition of the Grubbs' Catalyst

sample		r_1 (Å)	1_1 (Å)	poly disp.	vol. frac.
5[a]	before	23.4 ± 0.21	1054.7 ± 0.20	0.12 ± 0.012	
	after	1300.2 ± 76.89	80.8 ± 1.0	0.05 ± 0.006	
9[b]	before	18.02 ± 0.18		0.18 ± 0.0083	0.0021 ± 1.61 × 10^{-5}
	after	20.55 ± 0.21		0.17 ± 0.0083	0.0021 ± 1.56 × 10^{-5}

[a] Polydisperse cylinders model. [b] Schulz spheres, shielded coulomb model results.

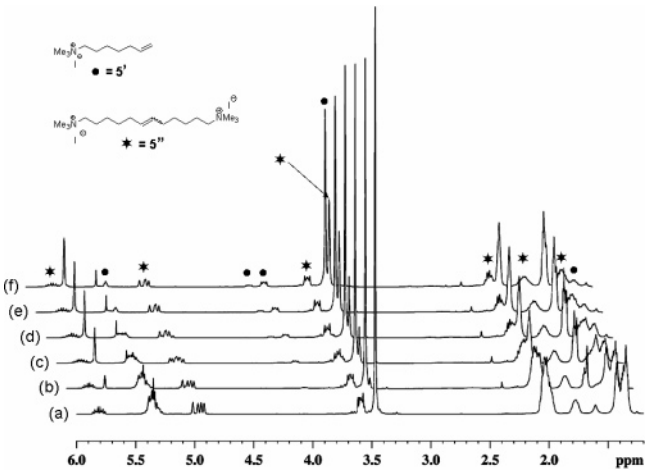

Figure 5. ^{1}H NMR decomposition of **5** in the presence of the second-generation Grubbs' catalyst in $CDCl_3$ (● = **5′**; ★ = **5″**); (a) 0 min, (b) 5 min, (c) 15 min, (d) 30 min, (e) 60 min, and (f) 120 min.

data obtained from both models is presented in Table 2 and is consistent with the predictions based on eq 1 above.

3. Surfactant Degradation. A. NMR Characterization. Demonstration of the metathesis degradative reactivity of **5** is shown in Figure 5. A chloroform solution of **5** in the presence of 2 mol % of the second-generation Grubbs catalyst[46] undergoes nearly complete decomposition of **5** within 60 min at 25 °C. Cyclohexene formation

Scheme 3. Observed Decomposition Products of 5

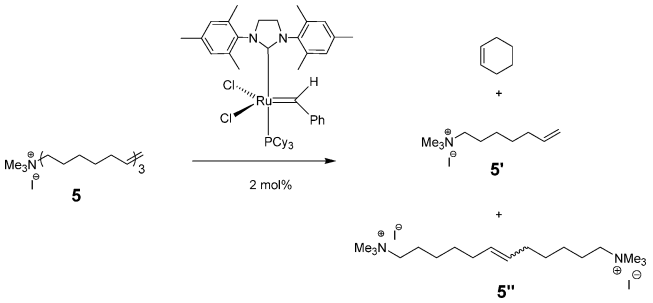

was clearly evident in the solution within five min of catalyst addition, as evidenced by the appearance of signals at δ = 1.62 and 1.97 ppm and a characteristic singlet at δ = 5.67 ppm. Chloroform extraction of the resulting aqueous solution indicates that cyclohexene was the only organic soluble product of the degradation.

^{1}H NMR spectroscopy also indicated the presence of the former headgroup remnant as 7-(*N*,*N*,*N*-trimethylammonium)hept-1-enyl iodide (unchanged chemical shift at δ = 3.48 ppm) as well as signals consistent with 1,-12-bis(trimethylammonium)dodec-6-enyl diiodide (equivalent methyls at δ = 3.43 ppm), likely resulting from ADMET coupling of two heptenyl iodide fragments (Scheme 3). This structural assignment is reasonable in light of terminal alkene generation in the presence of a metathesis catalyst and chemical shift comparison with independently prepared **5″** (prepared by catalytic coupling of trimethylammoniumheptenyl iodide **5′**, vide infra).

Bis-carboxylic acid **8** is stable up to 150 °C as detected by thermal gravimetric analysis; above this temperature,

(46) Scholl, M.; Ding, S.; Lee, C. W.; Grubbs, R. H. *Org. Lett.* **1999**, *1*, 953−956.

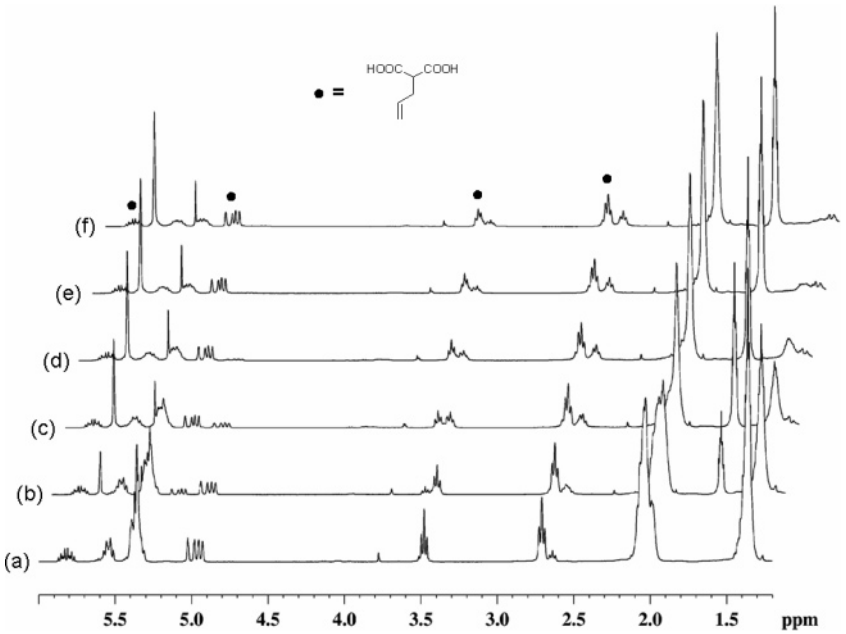

Figure 6. ^{1}H NMR decomposition of **8** in the presence of the second-generation Grubbs' catalyst in $CDCl_3$. (● = allyl malonic acid) (a) 0 min, (b) 5 min, (c) 15 min, (d) 30 min, (e) 60 min, (f) 120 min.

Scheme 4. Observed Decomposition Products of 8

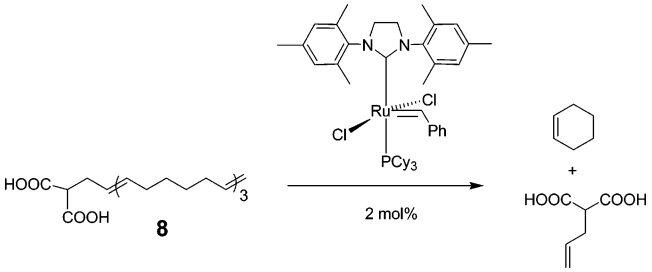

a single, distinct loss of 12% mass was seen, corresponding to clean mono-decarboxylation to the mono-carboxylic acid. Above 200 °C, **8** undergoes rapid mass loss from surfactant decomposition. However, in the presence of 2 mol % of Grubbs 2nd generation catalyst in chloroform, room-temperature decomposition of bis-carboxylic acid **8** is nearly complete within 60 min. Cyclohexene was again clearly present in solution within 5 min (Figure 6). Additionally, peaks assignable to allyl malonic acid (δ = 5.12−5.22 ppm, δ = 3.57 ppm, δ = 2.68 ppm) were present, by comparison with an authentic sample (Scheme 4).

One degradation pathway consistent with our ^{1}H NMR observations is illustrated in the idealized catalytic cycle depicted in Figure 7. Phosphine dissociation from the 16 electron complex $Cl_2(PCy_3)(L)Ru(=CHPh)$ (L = PCy_3, H_2-IMes) has been identified as a critical first step in the proposed mechanism of catalytic olefin metathesis.[47] Coordination of surfactant through either terminal or internal alkene to the reactive 14 electron intermediate **A**, followed by alkene−carbene coupling, would yield a surfactant-tethered metallacyclobutane intermediate capable of elimination of styrene to yield a surfactant-substituted Ru-alkylidene (catalytic cycle **I** in Figure 7). Intramolecular coordination of another alkene from the appended surfactant to the open metal coordination site in **B** could then lead to subsequent productive metallacyclobutane/alkylidene intermediates accompanied by elimination of cyclohexene (catalytic cycle **II**). Upon exhaustion of the alkenes in the aliphatic tail, a product mixture including surfactant-modified catalyst, cyclohexene and cross-metathesis products (from coupling with a second surfactant) would be expected.

Despite the insolubility of commercially available Grubbs catalysts in water, both ring-opening[48] and ring-closing[49] metathesis have been successfully performed under emulsion conditions in the presence of surfactants. The utility of RCM-degradable surfactant **5** in aqueous media was evident from surface tension and neutron scattering experiments on a degassed (dry nitrogen) 3 mM aqueous solution of **5** after introduction of 30 mol % of the second-generation Grubbs catalyst. Surface tension measurements taken over 28 h revealed that the micellar structure of the pristine solution was destroyed, as evidenced by an increase in the surface tension readings which ultimately approach that of water (Figure 8), indicating that none of the degradation products exhibit surface active behavior. In order to verify that there is no contribution to a reduced surface tension from the degradation products, the bromide salts of both 1-heptenyltrimethylammonium iodide **5′** and its cross-coupled derivative **5″** were prepared and their surface-active properties characterized by surface tensiometry. Dynamic surface tension values taken from aqueous samples of 1,12-bis(trimethylammonium)dodec-6-enyl dibromide as well as an authentic sample of 1-heptenyltrimethylammonium bromide at the same concentration, showed no depression of the surface tension of water. These results indicate that the metathesis depolymerization of **5** effectively eliminates the surface active properties of the surfactant entirely after 6 h, and the resultant products possess no surface active properties.

Neutron scattering measurements on identical samples of **5** (3 mM in D_2O) confirm the disruption of micellar organization as a result of catalyzed degradation. The data exhibits a marked change in the scattering profile over the entire q range. The model fit of the data indicates the formation of oblate cylindrical aggregates in solution,

(47) Grubbs, R. H., ed.; *Handbook of Metathesis*; Wiley: New York, 2003; Vol. 1, 112−131.

(48) Claverie, J. P.; Viala, S.; Maurel, V.; Novat, C. *Macromolecules* **2001**, *34*, 382−388.

(49) Davis, K. J.; Sinou, D. *J. Mol. Catal. A* **2002**, *177*, 173−178.

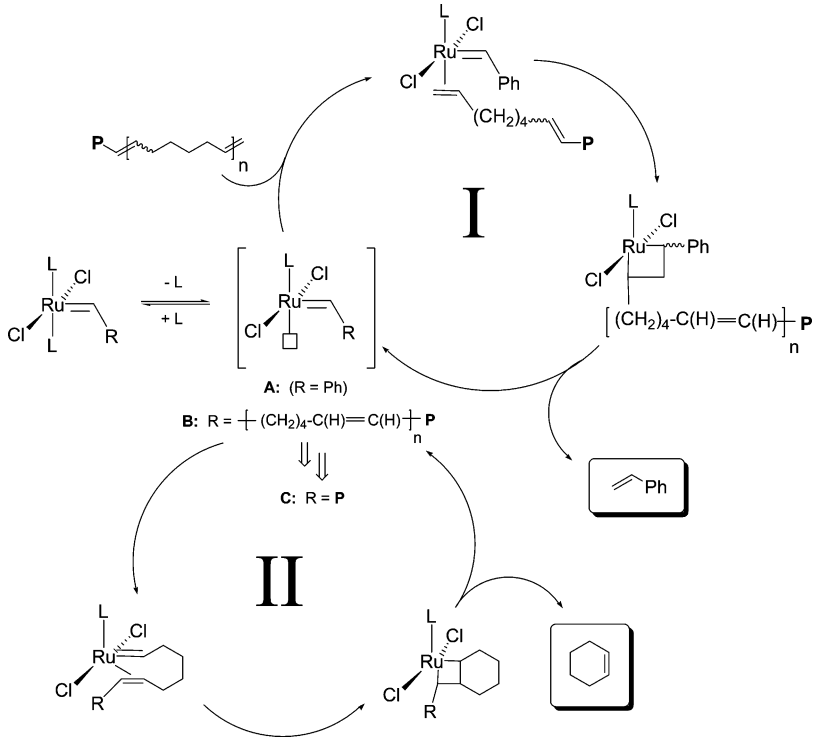

Figure 7. Proposed mechanism for the catalytic metathesis degradation of oligocyclohexenyl surfactants by ruthenium benzylidenes: R = Ph for initial catalyst (A), R = polar headgroup-terminated oligohexadiene (B), and ultimately headgroup-substituted alkylidene (C). P represents a generalized polar headgroup.

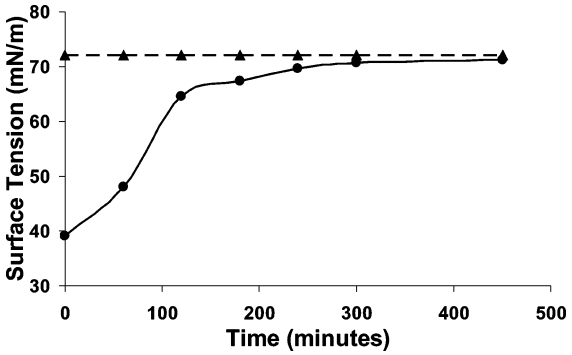

Figure 8. Decomposition of **5** by surface tensiometry (▲ = water baseline; ● = **5**).

with a radius of 1300.18 ± 76.89 Å. Although not identified, we believe these aggregates could be attributed to hydrophobic impurities derived from incomplete surfactant degradation, including the nonsurface active cross-coupled headgroups created by the Grubbs catalyst during metathesis depolymerization (i.e., the iodide analogues **5**′′).

In contrast to the clean degradation behavior of quaternary ammonium surfactant **5**, bis-carboxylate **9** apparently has a deactivating effect on the ruthenium catalyst. The inactivity of Grubbs catalyst toward degradation of **9** contrasts both with greater reactivity toward alkenes in the presence of free acids[50] and the metathesis activity displayed when the catalyst is allowed to act on free acid **8** (vide supra). One might suspect that chloride displacement at ruthenium with a coordinating anionic carboxylate could sequester the catalyst at the exterior micellar surface, slowing (or preventing) catalyst access to the unsaturated hydrophobic core, thereby attenuating the available catalyst concentration within the micelle. Another plausible scenario involves entropically favorable intramolecular or bridging chelation of the bis-carboxylate headgroup to ruthenium, yielding cationic ruthenium complexes whose ROMP activity has been demonstrated to be greatly reduced.[51]

Conclusions

We have designed and synthesized novel metathesis-active surfactants with regularly spaced C−C double bonds in their tails and demonstrated that they form well-behaved micelles in aqueous solution. The surfactants readily degrade into small and soluble molecules upon exposure to Grubbs olefin metathesis catalysts as illustrated by NMR, surface tensiometry, and SANS experiments in the first demonstration of ring closing metathesis applied to the degradation of a surfactant system. The major degradation product was identified as cyclohexene by ^{1}H NMR and mass spectral analysis. We continue to investigate conditions for metathesis depolymerization of anionic surfactants in aqueous media and are now investigating alternate surfactant headgroups as well as applying the surfactant to the synthesis of mesoporous materials in order to demonstrate their facile postsynthetic removal.

Acknowledgment. The authors thank Linda Breci at University of Arizona Mass Spectroscopy Facility and Ted Borek and Steven Meserole of the Materials Characterization Department at Sandia National Labs for their assistance in mass spectral analysis. This work was supported by the United States Department of Energy (US DOE) under Contract DE-AC04-94AL85000.

Supporting Information Available: Surfactant stability, SANS, and MM2 modeling results are available free of charge via the Internet at http://pubs.acs.org.

LA051438L

(50) Trnka, T. M.; Grubbs, R. H. *Acc. Chem. Res.* **2001**, *34*, 18−29.

(51) (a) Buchowicz, W.; Ingold, F.; Mol, J. C.; Lutz, M.; Spek, A. L. *Chem., Eur. J.* **2001**, *7*, 2842−2847. (b) Volland, M. A. O.; Hansen, S. M.; Rominger, F.; Hofmann, P. *Organometallics* **2004,** *23*, 800−816.